

High Volume Production of Pistons and Cups for Floating Cup Pumps and Motors

Robin F.H. Mommers¹, Johan G.J. Beijer², Peter A.J. Achten¹

INNAS B.V., Nikkelstraat 15, 4823AE Breda, The Netherlands¹

ART Group, Hermesstraat 8, 5047 TS Tilburg, The Netherlands²

E-mail: rmommers@innas.com, pachten@innas.com

In pumps and motors that are based on the floating cup type principle, the cylinder, or cup, is sealed by a line contact between the pistons and the cylinders. Due to the strict manufacturing tolerances that are required to obtain such a contact, and the high number of pistons and cups, the production costs of these components will make up a significant part of the production cost of the total machine. In an attempt to lower these costs, pistons and cups were formed from thick sheet metal, using multiple consecutive steps in a progressive die forming process. The advantage of such a process is that it can easily be automated and upscaled for mass-production.

A dedicated testbench was designed and used to measure the friction and leak flow at the line contact between the piston and the cup. Both traditionally manufactured components, and components that were made using the new process were tested. After determining optimal component specifications, a prototype floating cup type pump was equipped with the newly produced pistons and cups. A comparison shows, that this pump performs similar to a pump with traditional components. Therefore, the proposed production process appears to be a possible option for the production of less expensive pistons and cups, without decreasing the overall performance of the pump.

Keywords: mass-production, cost reduction, floating cup

Target audience: hydraulic component manufacturers, development engineers

1 Introduction

Floating cup type pumps and motors are hydrostatic piston machines, which means hydraulic fluid is moved by means of a piston that reciprocates inside of a cylinder. One of the main functions of a piston in any piston machine is to seal the cylinder chamber, in order to ensure that the chamber content cannot leave the cylinder during operation. In a floating cup type machine, the cylinder, or cup, is sealed by a line contact between the piston and the cup. This contact plays a crucial role in the low torque loss that such machines can achieve [1]. However, such a line contact also means that the leak path between the piston and cylinder is very short, potentially increasing the amount of leak flow rate.

The manufacturing tolerances that are required to obtain a decent line contact are found to be very strict [2], which means that pistons and cups are relatively expensive components. Furthermore, a typical floating cup type machine has 24 or more pistons and cups. As a result, the total production costs of these components will make up a significant part of the costs of the total machine.

Traditionally, the pistons and cups are manufactured from full material, using traditional machining techniques. In an attempt to lower the production costs of these components, an alternative production process is investigated in collaboration with the Dutch company ART. This company is specialized in making tools for high-end progressive stamping dies.

The goal of the current study is to determine whether it is possible to manufacture pistons and cups using a progressive die forming process. In such a process, components are formed from sheet metal using several consecutive die forming steps on an eccentric press. The advantage of such a process is that it can easily be automated and upscaled for mass-production.

2 Component design

This study focusses on a piston and cup for a prototype 45 cc floating cup pump. On the left of fig. 1a, a cross-section of the current piston and cup is shown. In the actual pump, the piston (shown in orange) is fixed to a rotating axle by means of a bolt (shown in gray), and a piston nut (shown in lighter orange). In the figure, the cup (shown in green) is pushed upwards as a result of oil pressure inside the cup. An angled plane behind the cup base ensures that the cup sits at a swash angle (8° in this case). Since the top of the piston is of a spherical shape, the cup can pivot around the piston. The cup itself is not fixed but "floating" (i.e. it can move freely along the plane). The spherical piston shape determines the position of the cup on the angled plane.

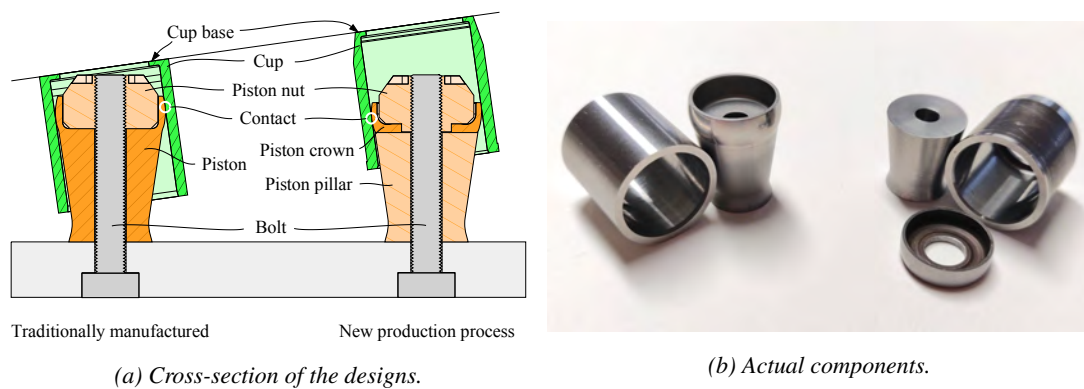


Figure 1: Comparison between the traditionally manufactured components and the new components.

2.1 Material deformation

The contact between the piston and cup is crucial for the performance of the pump. In fig. 1a, the location of the contact is highlighted with small white circles. Passing through these points, there is a full circular line contact between the piston sphere and the inside of the cup, parallel to the angled plane. When the piston moves back and forth inside the cup, the location of the contact line on the piston will remain the same, while the location of the contact on the cup will move along the inside of the cup. During operation, there will be pressurized oil inside of the cup, which will lead to material deformation of both the piston and the cup [2, 3]. At any piston position, the deformation of the cup should be more or less equal to the deformation of the piston. If this is not the case, it can lead to:

- high friction losses, for example, when the piston sphere radius expands more than cup radius, the piston will exert a contact force on the inside of the cup, or
- high leakage losses, for example, when the cup radius expands more than the piston radius, there will be a gap between the two components.

An important part of the current study is to determine the manufacturing tolerances on the piston and cup that are required for an optimal contact between the two deformed components during the full piston stroke, at all possible pressure levels.

2.2 Design changes

The solid shape of the traditional design of the piston (left of fig. 1a) will be impossible to manufacture using a progressive die forming process. Therefore, the right side of fig. 1a shows a cross-section of a new piston design. The main difference is that the piston is split into a piston crown (darker orange) and a piston pillar (lighter orange). In this case, the spherical shape is now found on the piston crown, while the piston pillar only functions as a base for the crown to rest on. Note that the material thickness of the piston crown makes it possible to produce this shape using a stamping process.

Next to the design of the piston, the design of the cup also differs from the traditional design. The main difference is found in the design of the cup base. Due to the additional material at the base of the cup, the stiffness of the cup is higher near the cup base. As a result, the material deformation of the cup will not be equal for every position of the piston. In order to reduce this stiffness, some material is removed from the inside of the traditional cup. However, this is not possible in die forming, as the formed parts need to be releasing. This is why in the new design, material is removed from the outside of the base of the cup. Figure 1b shows a picture of the produced components.

3 Production process

For this project, ART has developed a production process for both the piston and the cup, which consists of multiple consecutive die forming steps, or phases. Each step has a specific product deformation mechanism, with processes like deep drawing, coining, bending, cutting or wiping. Some steps are a combination of these different mechanisms. In an actual production machine, all of the tools required for each step are placed in series on a single press. This means that all steps are performed simultaneously with each punch of the press. After a punch, the products will automatically be transported to the next step of the process. It is estimated that the designed process can be used to output about 60 to 100 products per minute.

To validate the developed process, a prototyping crank driven eccentric press was used which could perform only one step of the full process at a time. Figure 2 shows this press, which is equipped with the tool to perform the first phase of the cup production process. This first phase can be characterized as a deep drawing step. After each phase, the resulting product was inspected to see if everything went as expected. When the phase was completed for all products, the press was reconfigured to perform the next step of the process.

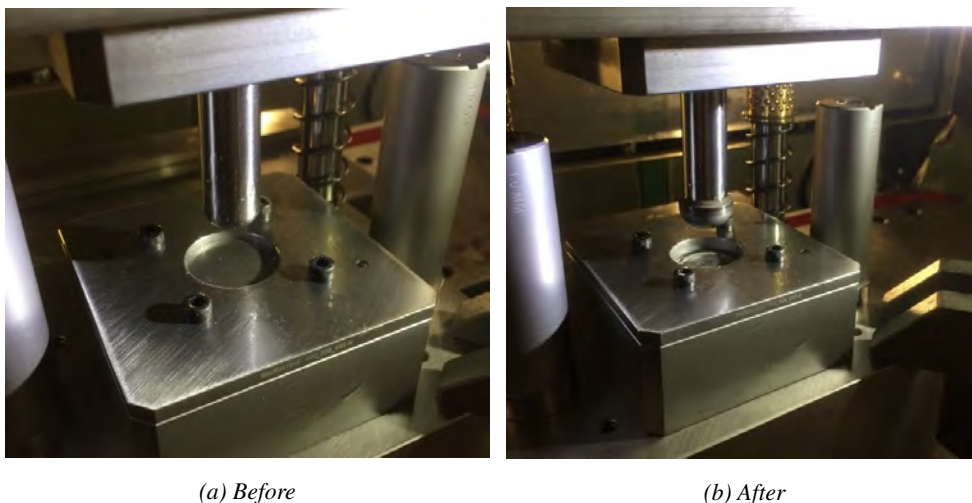


Figure 2: First phase (deep drawing) of the production process of the cup on a prototyping press.

3.1 Cup

The process for producing cups starts with a circular piece of thick sheet metal. Since the cup is a relatively tall product, a high deep drawing ratio is required to achieve the total length. Figure 3 shows the product after each of the production phases, starting with the circular piece of metal on the left, and ending with the final product on the right.

During this stage of the process development, it was assumed that the final product would need some post-process machining to reach the right tolerances. Therefore, the inner radius of the cup was intentionally made slightly smaller than the design specifications. This final product was hardened and then machined to meet the specified tolerances using more traditional manufacturing techniques. Further development of the production process and hardening process is expected to result in a final product that is much closer to, or within the specified tolerances. Since this development could take several years, this is outside of the scope of the current study.



Figure 3: Cup after the different phases of the production process.

3.2 Piston

Figure 4 shows the product after the different phases of the production process for the pistons. Similar to the process for the cups, this process starts with a circular piece of metal on the left, and ends with the final product on the right. Similar to the cup, this final product also needs some post-process machining.

As was mentioned before, the piston in a floating cup pump has a spherical shape. While it could theoretically be possible to produce this shape in a consistent way, this would also require much more development. For now, the radius of the piston crown was made slightly too large and the spherical shape was machined post-process.

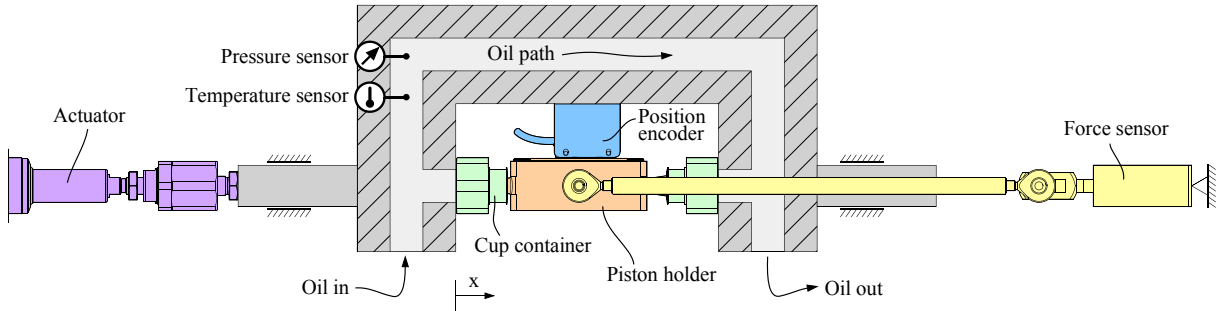


Figure 4: Piston after the different phases of the production process.

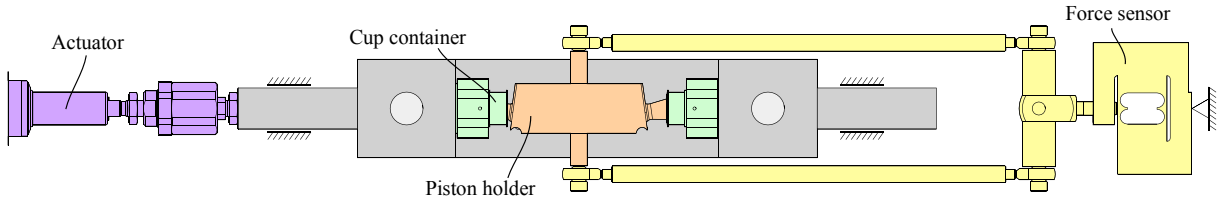
4 Individual piston and cup test

4.1 Testbench

A separate testbench was designed to compare the friction and leak flow at the line contact between a single piston and cup. Figures 5a and 5b show a drawing of the testbench containing all relevant parts, while fig. 6 shows a picture of the actual testbench. The testbench, as it is shown here, can be separated into a stationary group and a moving group. The stationary group consists of the piston holder (shown in orange) and the force sensor (shown in yellow). Two pistons are mounted on opposite sides of the piston holder, while two rods connect the holder to the force sensor that is fixed in place. The moving group consists of an actuator (part of which is shown in purple), a steel frame (shown in gray), a position encoder (shown in blue), and two cup containers (shown in green). Specifications about the used sensors can be found in the appendix.



(a) Top view, with cross-section of the steel frame, showing the path of the oil.



(b) Front view.

Figure 5: Sketch of the testbench for testing individual pistons and cups viewed from top (a) and front (b). The actuator (purple) moves the steel frame (gray) including the cup containers (green) and position encoder (blue) in the direction of x , while the piston holder (orange) is kept stationary by the force sensor (yellow).

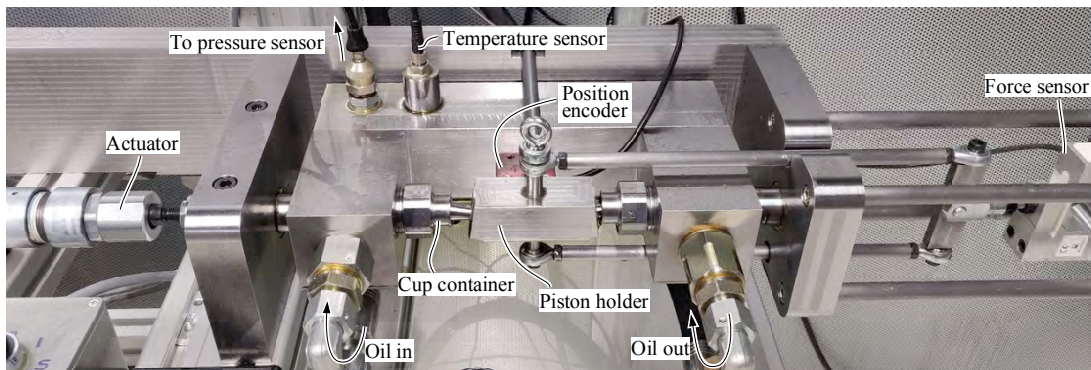


Figure 6: Picture of the actual testbench.

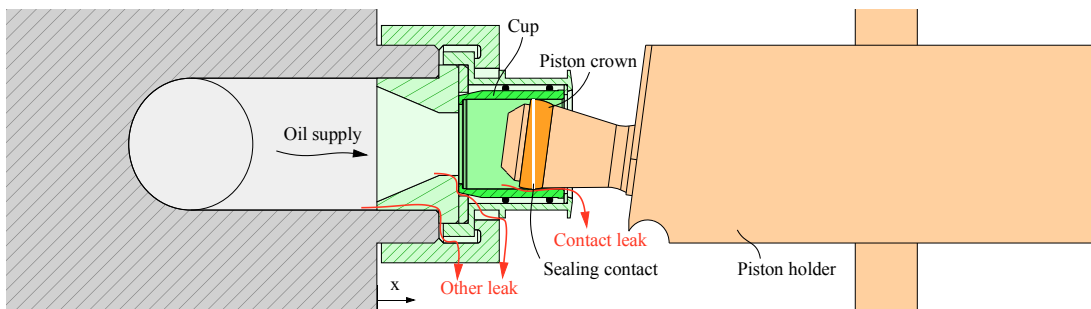


Figure 7: Cross section of the cup container, showing the cup, the piston, and the sealing contact between these two components. The red arrows show three leak paths.

The steel frame is guided by two sliding bearings, which means that the attached actuator can only move the frame in the horizontal direction, as is indicated with the x in the figure. On both sides of the piston holder, a cup container is fixed to the steel frame. Furthermore, the position encoder is also fixed to the steel frame and is placed at a small distance from a magnetic encoder scale that is attached to the piston holder. Since the encoder itself is moving relative to the scale, the position of the frame with respect to the piston holder can be measured.

Figure 5a shows a cross-section of the steel frame, in which a path is made for the oil to flow through. During a measurement on this testbench, an oil flow is directed into the steel frame, and out of the frame on the other side (oil in and oil out in figs. 5a and 6). The pressure and temperature of this oil is monitored using two sensors, which are connected to the oil path. During all of the measurements, the temperature of the oil is kept between 49°C and 51°C.

Oil can also flow in and out of the cup via the cup containers. Figure 7 shows a cross-section of the cup container (again in green), which consists of several separate components. These components ensure that the cup itself (highlighted green part) is held in place. The bottom of the cup is connected to the oil path in the steel frame, which means that oil can reach the inside of the cup.

The piston holder (again in orange) is also shown in fig. 7. The piston crown (highlighted orange part) is placed in a way that is similar to the way it is found inside of an actual floating cup pump. The contact between the piston and cup is highlighted with the white line. When the actuator moves the gray frame in the direction of x , the cup will move forward, and the sealing between the piston and the cup will move towards the base of the cup, as it would in an actual pump.

4.2 Tested components

The main goal of the individual piston and cup tests is to find out how the contact between the piston and the cup affects the performance of the full pump. To this end, a small number of pistons and cups were produced using the new production process. These components were then machined at slightly different radii. The average radius of the inside of these cups, and the average radius of piston spheres was measured.

Table 1 shows the measured radii of some of these components. The difference between the measured average radius and the base radius of 6.8 mm is indicated with ΔR which is given in μm . The different combinations of pistons and cups will result in different gap sizes between the two components, as is shown in the table. For example, the average of the inside radius of Cup 1 is 6.8007 mm, so ΔR is $+0.7 \mu\text{m}$. The average radius of the sphere of Piston 1 is 6.7989 mm, so ΔR is $-1.1 \mu\text{m}$. When these two components are combined on the testbench, there will be a total average radial gap of $1.8 \mu\text{m}$. Furthermore, this combination will be referred to as PIC1 (Piston 1 combined with Cup 1).

Table 1: Average difference in radius (ΔR) of three new pistons, two new cups, and two traditional sets of pistons and cups, with respect to a base radius of 6.8 mm. The values inside of the table indicate the radial gap between the two components ($\Delta R_{cup} - \Delta R_{piston}$). All values are given in μm .

Manufactured using new process					Traditional sets			
	Average ΔR	Piston 1	Piston 2	Piston 3		Average ΔR	Piston A	Piston B
		$-1.1 \mu\text{m}$	$-0.7 \mu\text{m}$	$+0.7 \mu\text{m}$			$+0.2 \mu\text{m}$	$+0.1 \mu\text{m}$
Cup 1	$+0.7 \mu\text{m}$	1.8	1.4	0.0	Cup A	$+0.3 \mu\text{m}$	0.1	
Cup 2	$+1.4 \mu\text{m}$	2.5	2.1	0.7	Cup B	$+0.3 \mu\text{m}$		0.2

Apart from several of the combinations shown in the left of tab. 1, two sets of traditionally manufactured pistons and cups were tested as well. The results from these measurements will act as a baseline for comparing the other sets. Since these pistons and cups will not be interchangeable, they are referred to as Set A and Set B. Please note that the radial gaps of the traditional sets (0.1 and 0.2 μm) are smaller than the radial gap of most of the combinations with components from the new production process (0.0-2.5 μm). The deformation of the new piston and cup design, as a result of oil pressure in the cup, is different from the deformation of the traditional designs. As a result, the optimal gap size of the new components is found to be larger than the gap size of Set A and Set B, as will be described in the following sections.

4.3 Friction test

The tested pistons have a radius of 6.8 mm. This means that at an oil pressure of 400 bar, the piston shown in fig. 7 will be pushed out of the cup with a force of 5.8 kN. When the frame is moving relatively slow, the piston on the opposite side of the piston holder is pushed out with the same amount of pressure and force (fast movement will result in a pressure difference between the two pistons, due to flow restrictions between the cup and the steel frame). Therefore, the net force on the piston holder is zero, which means the only forces that remain are the friction force at the contact between both pistons and cups. These forces are measured by the force sensor. Since we are interested in the performance of only one piston-cup contact, the piston on the other side of the piston holder is chosen such that the contact will have little to no friction (i.e. relatively large gap between piston and cup, which will give high leakage but low friction).

In the actual pump, high operating speeds will also introduce additional forces that can have an effect on the friction between the piston and the cup (e.g. centrifugal forces, or friction between the base of the cup and the angled plane). In the current testbench, it is not possible to account for these additional forces. Furthermore, friction between the piston and the cup is expected to be largest at a low operating velocity due to coulomb friction (instead of viscous friction that will occur at higher operating speeds). Therefore, the friction force is measured while the steel frame is actuated back and forth during a period of 60 seconds, at a velocity of 3 mm/s (corresponds to 8 rpm of the pump). The distance that the piston travels during these tests is equal to the distance it makes inside of the actual pump.

Figure 8a shows the measured friction force of the traditional sets, as well as three combinations from tab. 1 at 200 bar. Please note that the y-axis in this figure is split into three parts. The figure shows that the combination

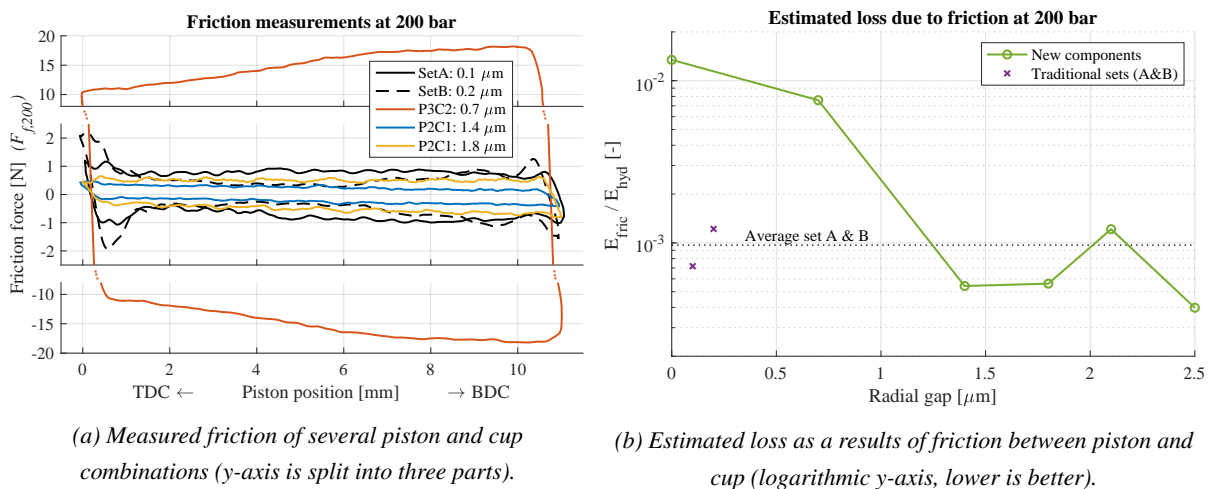


Figure 8: Friction measurements of several piston and cup combinations at 200 bar (Shell Tellus46 at 50°C).

with a radial gap 1.4 and 1.8 μm had similar levels of friction as the traditional combinations (which had a smaller gap). However, the piston and cup with a radial gap of 0.7 μm had significantly more friction than the other combinations. This is most likely caused by the deformation of the piston crown with respect to the deformation of the cup. From the results shown here, it appears that there is a minimum gap size that needs to be achieved between the piston and the cup to ensure low friction. When the gap size is decreased to below this minimum, the friction will increase very rapidly.

The relation between force and the piston position can be used to estimate the amount of energy loss as a result of friction between the piston and the cup. A standard pump cycle can be split into two phases:

- supply: cup is connected to low pressure port (pressure p_1), piston is moving from top dead center (TDC, around 0 mm in fig. 8a) to bottom dead center position (BDC, around 11 mm in fig. 8a)
- discharge: cup is connected to high pressure port (pressure p_2), piston is moving from BDC to TDC.

For a linear movement, the energy consumption can be found by integrating the force with respect to the position. The hydraulic energy, E_{hyd} , for a piston is thus found to be:

$$E_{hyd} = \int (pA_p) dx = A_p \left[\int_{TDC}^{BDC} p_1 dx + \int_{BDC}^{TDC} p_2 dx \right] = A_p (p_1 - p_2) \Delta x \quad (1)$$

with pressure p , surface area A_p , and Δx the distance between TDC and BDC. The pump in which the tested pistons and cups will be implemented, typically has a supply pressure of 4 bar. Since no friction measurements were conducted at this pressure level, it is assumed that the friction during the supply phase will be similar to the friction that was measured at 50 bar ($F_{f,50}$). The energy loss as a result of friction, E_{fric} , is found to be:

$$E_{fric} = \int_{TDC}^{BDC} F_{f,50} dx + \int_{BDC}^{TDC} F_{f,p_2} dx \quad (2)$$

with F_{f,p_2} the friction force measured at pressure level p_2 (as shown in fig. 8a for 200 bar). This integration was done numerically using the measured friction forces. The ratio between friction energy and hydraulic energy (E_{fric}/E_{hyd}) can be seen as an estimation of the efficiency loss as a result of friction between the piston and cup.

Figure 8b shows the estimated friction loss as a function of the gap size between the piston and cup, at 200 bar. The result is similar to the results from fig. 8a: a radial gap of less than 1 μm results in significantly higher friction losses than the traditional sets. A radial gap larger than 1 μm results in comparable or less friction loss. Although it is expected that a larger gap will result in a lower friction force, fig. 8b does not show a clearly decreasing trend at radial gaps larger than 1.5 μm . Since the friction is already very low for these combinations, small stochastic differences in surface roughness can have an influence on the measured friction. Such differences seem to cause the slightly larger losses that were measured for the combination with a radial gap of 2.1 μm .

4.4 Leak test

The cross-section in fig. 7 shows three leak paths, through which high pressure oil can leave the cup container during measurements on the testbench. One of these paths is along the sealing contact between the piston and cup ("contact leak" in the figure). This oil will leak out of the cup during operation. The two "other leak" paths are between other components of the cup container and can leak via several leak holes. During the leak test, the piston is kept stationary for 60 seconds, at incremental positions inside of the cup. During these 60 seconds, the oil that leaks via the sealing contact is caught in a beaker. The other leak flows are directed away from this beaker. By weighing the beaker, the amount of oil that has leaked via the sealing contact during 60 seconds can be measured and converted into a flow rate using the mass density of the oil (855.1 kg/m^3 was used here, for oil at 0 bar, 50°C).

Figure 9a shows the measured leak flow rate of several of the tested combinations at different positions in the cup, at 200 bar. In general, this figure shows that each of the combinations has a relatively small leak flow rate near

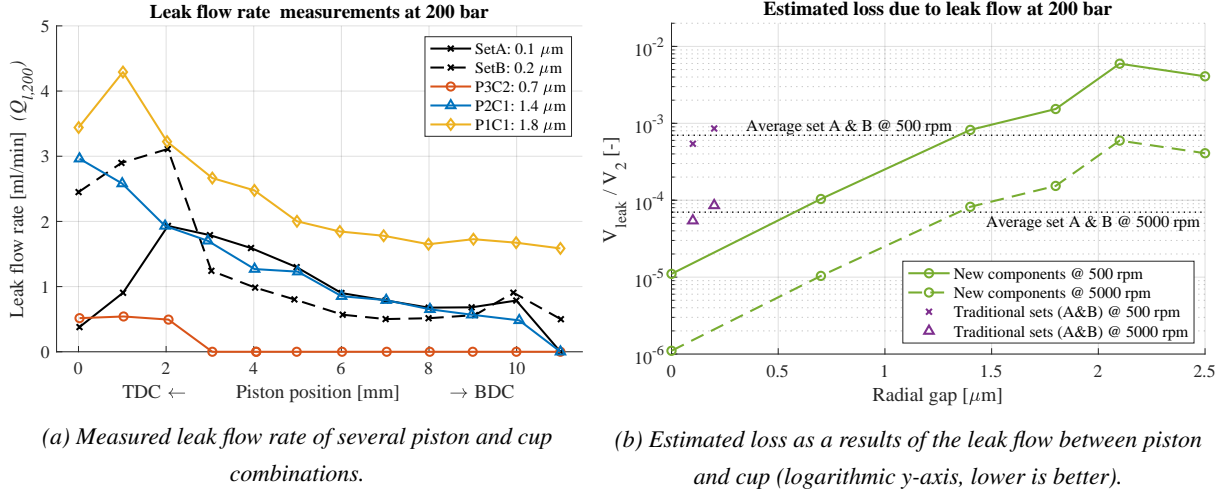


Figure 9: Leak measurements of several piston and cup combinations at 200 bar (Shell Tellus46 at 50° C).

BDC. When the piston moves closer to TDC, leak flow increases. The components with a radial gap of 1.4 μm had a very similar amount of leak flow as the two traditional sets. The other two components performed as expected: a larger gap resulted in more leak flow, while a smaller gap resulted in less leak flow. The combination with a radial gap of 0.7 μm even did not leak a single drop of oil during the 60 seconds of the measurement, for most part of the piston stroke.

During the discharge phase of the pump cycle, a certain amount of volume is pushed out of the cup. If commutation is ignored, the total discharge volume, V_2 , is the product of the piston surface area and the full piston stroke:

$$V_2 = A_p \Delta x \quad (3)$$

Due to the leak flow at the sealing contact between the piston and the cup, part of V_2 will flow into the pump housing instead of the discharge line. If the pump is operated at a rotational velocity ω , the piston position x can be described as a function of time t :

$$x(t) = \frac{\Delta x}{2} (1 - \cos(\omega t)) \quad (4)$$

Note that the piston is in BDC at time $t_B = \pi/\omega$, and in TDC at time $t_T = 2\pi/\omega$. Using linear interpolation between the measured piston positions shown in fig. 9a, eq. (4) is used to estimate leak flow during the discharge phase of the pump cycle. At pressure p_2 , this flow rate is described by Q_{l,p_2} , which is a function of the piston position $x(t)$. The total amount of volume that is estimated to leak during the discharge phase of the pump cycle, V_{leak} , can be found by integration of the flow rate:

$$V_{leak} = \int_{t_B}^{t_T} Q_{l,p_2}(x(t)) dt \quad (5)$$

Since the difference between the supply pressure and the pressure in the pump housing will be very small, it is assumed that there is no leak flow between the piston and the cup during the supply phase of the pump cycle. The ratio between the leaked volume and the discharge volume (V_{leak}/V_2) is an estimation of the efficiency loss as a result of leakage between the piston and cup.

Figure 9b shows the estimated efficiency loss due to leakage as a function of the size of the gap between the piston and cup, for a rotational speed of 500 and 5000 rpm. At 5000 rpm, the piston empties the cup in 0.006 s, which is ten times faster than it does at 500 rpm. The leaked volume during this time is thus also ten times smaller, which

is why the difference between total estimated losses due to leak flow between the two velocities is also a factor of ten. It can be found that a radial gap that is larger than $1.5 \mu\text{m}$ results in more leak flow losses than the traditional components, while a smaller gap is estimated to result in less leak flow losses.

4.5 Combined loss

The results from the friction test (fig. 8b) and the leak test (fig. 9b) can be combined into a total estimated loss. Figure 10 shows this combined loss relative to the mechanical input power at two different rotational velocities. The figures show the loss as a function of both the radial gap between the piston and cup, and the discharge pressure level. As was mentioned before, friction loss is lower for piston and cup combinations with a larger radial gap, while leak loss is lower for combinations with a smaller gap. As a result, there is an minimum total amount of loss somewhere in the middle. Figure 10a shows that at a rotational velocity of 500 rpm, a radial gap around $1.5 \mu\text{m}$ will be optimal. At larger rotational speeds, the effect of the leak losses will become smaller. As a result, fig. 10b shows that at 5000 rpm the radial gap can be larger than $1.5 \mu\text{m}$ without expecting high losses. Since the pump will need to run efficiently at the full range of rotational velocities, it seems best to select pistons and cups with a radial gap between 1 and $2 \mu\text{m}$.

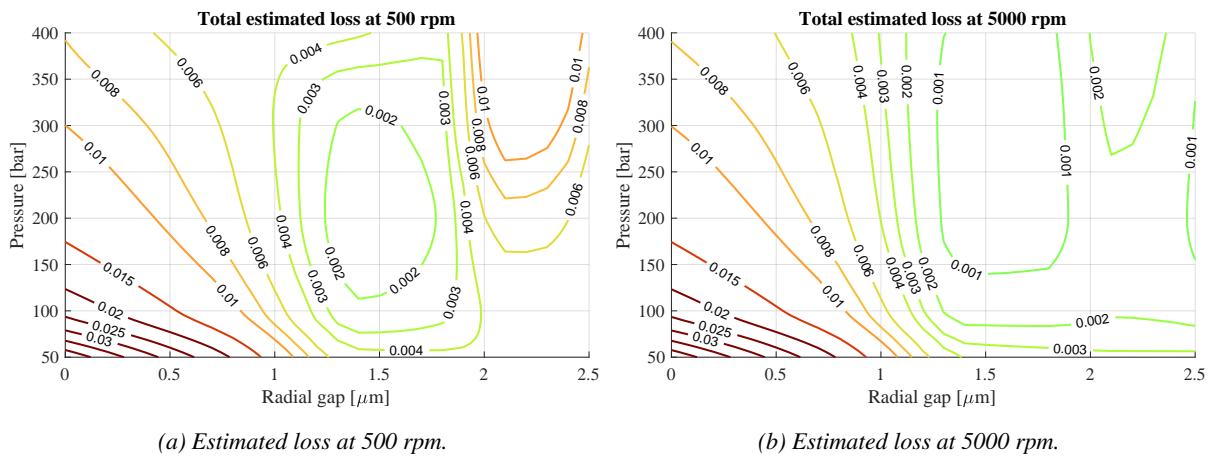


Figure 10: Estimated total loss as a function of gap size and pressure levels (lower is better).

5 Complete pump test

It is important to note that the testbench was designed to emulate the most predominant operating conditions of the pistons and cups in a floating cup pump. However, it is clear that the operation in the testbench is not the same as in an actual pump, and there are still a lot of uncertainties when it comes to the performance of the new pistons and cups. The only way to measure the actual performance of the new components is to compare measurements between a pump with traditional pistons and cups and a pump with new pistons and cups. Therefore, a larger batch of components was produced using the new production process. Following the results of the analysis shown above, these pistons and cups were machined post-process to have a radial gap between 1 and $2 \mu\text{m}$.

5.1 Measurement setup

The results presented below compare measurements that were conducted on a 45 cc prototype floating cup pump. This pump was first equipped with traditionally manufactured pistons and cups, and then with the pistons and cups that were produced using the new production process. Apart from these components, the two measured pumps were identical. The pumps were measured on the Innas testbench [4], in accordance with ISO4409 [5]. During

this measurement, the supply pressure is set to 4 bar, and the pump is operated at all different combinations of the following operating conditions:

- operating speeds: 500, 1000, 1500, 2000, 2500, 3000, 3500 rpm, and
- discharge pressures: 50, 100, 200, 300, 400 bar

The difference between the pump with the traditionally manufactured pistons and cups and the pump with the new pistons and cups is discussed by looking three parameters: leak flow rate, torque loss, and efficiency. The leak flow rate is measured directly by a flow sensor. The torque loss and overall efficiency of the pumps are calculated using the output of several sensors [6]. Specifications about the used sensors can be found in the appendix.

5.2 Results

Figure 11a shows a comparison of the measured external leak flow rate. In this figure, the results of the pump with the traditional components is shown with the dashed lines, while the results of the pump with the new pistons and cups is shown with the solid lines. The different colors and markers indicate the measurements at different discharge pressures. Looking at the 100 bar measurements, it is found that the leak flow rate at different operating speeds is almost identical between the two pumps. However, as the pressure increases the pump with the new components has significantly less leakage. Since the only differences between the configuration of the two pumps are the pistons and cups, it is very likely that the reduced leak flow rate is caused by the changes that were made to the design of these components.

Figure 11b shows the calculated torque loss of the two pumps. The results are presented similarly to the leak flow rate results. The figure shows that there is almost no difference between the torque loss of the two pumps. The 100, 200, and 300 bar measurement all have the same amount of torque loss, which is why these lines are almost indistinguishable from each other. Only at 400 bar, the torque loss of the pump with the new pistons and cups was found to be slightly less than the torque loss of the pump with the traditionally manufactured components.

Figure 12 shows the overall efficiency of the two pumps. These results are presented in the form of a contour plot, in which the values between measured operating points are estimated using interpolation. Within the measured range, it is found that the performance of the two pumps is fairly similar. At higher operating pressures, the pump with the new pistons and cups even achieved a slightly higher efficiency. This is mainly caused by the decreased leak flow rate at high operating pressures, as shown before.

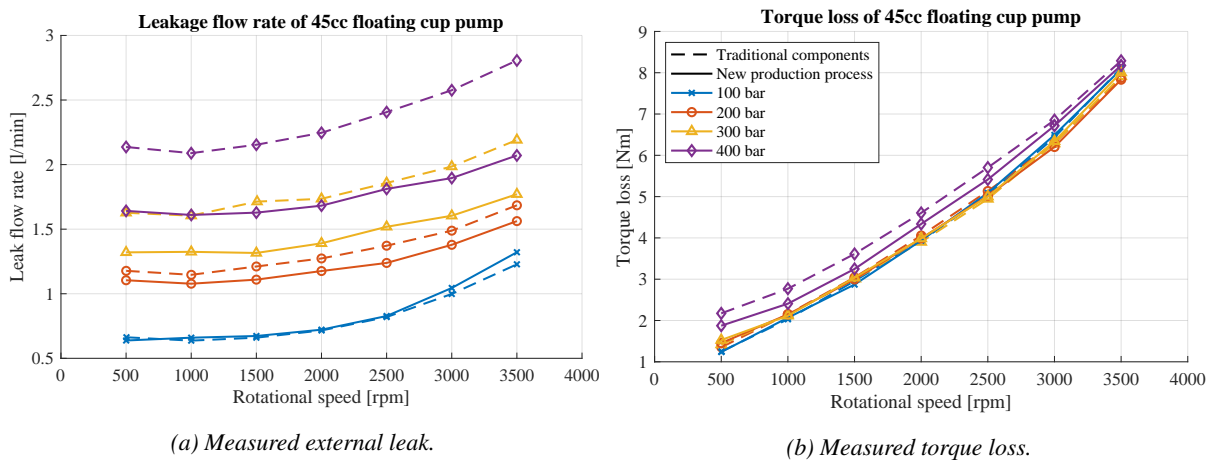


Figure 11: Performance measurements of the prototype 45 cc floating cup pump with traditionally manufactured components (dashed lines) and pistons and cup that were made using the new production process (solid lines).

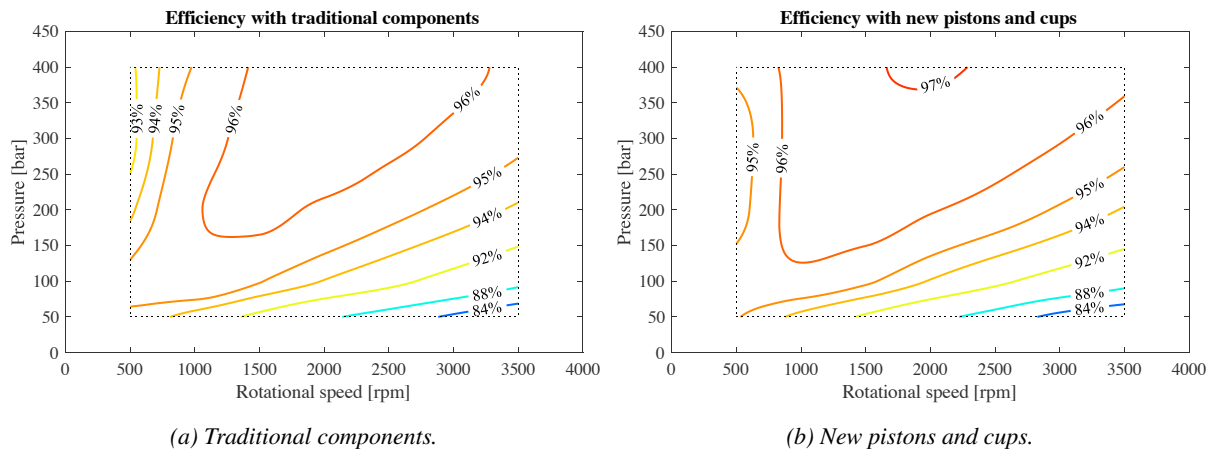


Figure 12: Efficiency field of the prototype 45 cc floating cup pump with traditionally manufactured components (a) and pistons and cup that were made using the new production process (b).

6 Conclusion

To reduce the production cost of pistons and cups for hydrostatic machines based on the floating cup principle, an alternative production process was designed and evaluated. For both the piston and the cup, this process consists of several sequential phases on an eccentric press. In an actual production machine, such a process is expected to produce 60 to 100 products per minute. Currently, the final products of this new production process are machined post-process to meet the required tolerances. This study therefore serves as a proof of concept. Further development of the production process is expected to result in a final product that is much closer to or within the specified tolerance.

The new process was first used to manufacture a range of products with slightly different radii. Experimental data showed that a combination of a piston and a cup with a radial gap of 1 to 2 μm performed best in terms of minimal leakage and friction losses. As a result, a larger batch of pistons and cups was produced with this specification, to equip a prototype 45 cc floating cup pump. The performance of this pump was measured and compared to the same pump with traditionally manufactured pistons and cups. Overall, the results of these measurements showed that the two pumps performed similarly. It is therefore concluded, that the proposed production process appears to be a possible option for the production of less expensive pistons and cups, without decreasing the overall performance of the pump.

Acknowledgements

The results described in this paper were achieved in an MIT Zuid R&D project of Innas BV and ART Group, which was partly funded by the Ministry of Economic Affairs and Climate Policy and the province Noord-Brabant, The Netherlands.

References

- [1] Achten, P., Potma, J., and Achten, J. Low speed performance of axial piston machines. In *Fluid Power Systems Technology*, volume 51968, page V001T01A014. American Society of Mechanical Engineers, 2018.
- [2] Achten, P. A. J. Volumetric losses of a multi piston floating cup pump. In *Proceedings of the National Conference on Fluid Power, Las Vegas, USA*, volume 50, page 337, 2005.

- [3] Achten, P. A. J., Mommers, R. F. H., Potma, H. W., and Achten, J. J. Design and testing of pistons and cups for large hydrostatic pumps and motors. In *12th International Fluid Power Conference, 12. IFK, Dresden, Germany*, page 79, 2020.
- [4] Achten, P., Potma, J., and Eggenkamp, S. A new hydraulic pump and motor test bench for extremely low operating speeds. In *ASME/BATH 2017 Symposium on Fluid Power and Motion Control*. American Society of Mechanical Engineers Digital Collection, 2017.
- [5] ISO4409:2019. *Hydraulic fluid power, positive displacement pumps, motors and integral transmissions; Methods of testing and presenting basic steady state performance*. International Organization for Standardization, 2019.
- [6] Achten, P., Mommers, R., Nishiumi, T., Murrenhoff, H., Sepehri, N., Stelson, K., Palmberg, J.-O., and Schmitz, K. Measuring the losses of hydrostatic pumps and motors; a critical review of iso4409:2007. In *BATH/ASME 2019 Symposium on Fluid Power and Motion Control*. American Society of Mechanical Engineers, 2019.

Nomenclature

Variable	Description	Unit
ΔR	Radial difference with respect to a base radius (6.8 mm in this study)	[m]
Δx	Distance between top and bottom dead center positions	[m]
ω	Rotational velocity	[rad s ⁻¹]
A_p	Surface area of piston	[m ²]
E_{fric}	Energy loss due to friction	[J]
E_{hyd}	Hydraulic energy	[J]
$F_{f,p2}$	Friction force at pressure p_2	[N]
p_1	Pump supply pressure	[Pa]
p_2	Pump discharge pressure	[Pa]
$Q_{l,p2}$	Leak flow rate at pressure p_2	[m ³ s ⁻¹]
t	Time	[s]
V_2	Discharge volume of a single piston	[m ³]
V_{leak}	Leak volume	[m ³]
x	Piston position	[m]

Appendix

Sensor information

Specifications of the sensors used in the individual piston and cup testbench, as described in section 4:

Measured quantity	Sensor	Range	Accuracy
Friction force	HBM S2M/100N	-100 to 100 N	± 0.02 N
Oil pressure	Honeywell STJE 7500 psig	0 to 517.1 bar	± 0.259 bar
Oil temperature	Testo type 13 PT100 class B	-50 to 400°C	± 0.3 °C
Resolution			
Piston position	RLS LM13IC10BCB	incremental	1.953 μm
Weight leak flow	Kern PLJ 720-3A	720 g	1 mg

Specifications of the sensors used during the complete pump measurements, as described in section 5:

<i>Measured quantity</i>	<i>Sensor</i>	<i>Range</i>	<i>Accuracy</i>
Torque	Kistler 4541A / 4550A500	-500 to 500 Nm	±0.25 Nm
Supply pressure	Honeywell TJE 500 psig	0 to 34.5 bar	±0.035 bar
Discharge pressure	Honeywell STJE 7500 psig	0 to 517.1 bar	±0.259 bar
Case (leak) pressure	Omega PXM02MD0-040BARGV	0 to 40.0 bar	±0.02 bar
Discharge flow rate	VSE RS 400/32	1.0 to 400 l/min	0.5% MV*
External leak flow rate	VSE VSI 0.1/16	0.01 to 10 l/min	0.3% MV*
Oil temperature (3x)	Testo type 13 PT100 class B	-50 to 400°C	± 0.3 °C
			<i>Resolution</i>
Rotational speed	Kistler 4541A / 4550A500		60 pulses/rev

* accuracy for this sensor is defined as a percentage of the measured value (MV)